

## Hydroxypropyl Methylcellulose Acetate Succinate-Based Spray-Dried Dispersions: An Overview

Dwayne T. Friesen,<sup>\*,†</sup> Ravi Shanker,<sup>‡</sup> Marshall Crew,<sup>†,§</sup> Daniel T. Smithey,<sup>†,§</sup>  
W. J. Curatolo,<sup>‡</sup> and J. A. S. Nightingale<sup>†</sup>

Bend Research Inc., 64550 Research Road, Bend, Oregon 97701, and Pfizer Inc.,  
Global R&D, World Wide Pharmaceutical Sciences, Groton, Connecticut 06340

Received July 1, 2008; Revised Manuscript Received October 10, 2008; Accepted October 13, 2008

**Abstract:** Spray-dried dispersions (SDDs) of low-solubility drugs have been prepared using the polymer hydroxypropyl methylcellulose acetate succinate (HPMCAS). For a variety of drug structures, these SDDs provide supersaturation in *in vitro* dissolution determinations and large bioavailability increases *in vivo*. In bile-salt/lecithin *in vitro* solutions, these SDDs provide amorphous drug/polymer colloids and an increased concentration of free drug and drug in micelles relative to crystalline or amorphous drug. As dry powders, the SDDs are a single amorphous phase in which the drug remains amorphous and dispersed and does not crystallize over storage times relevant for practical drug products. A melting temperature ( $T_m$ )/glass-transition temperature ( $T_g$ ) (K/K) versus log  $P$  map for 139 compounds formulated as SDDs provides a perspective on an appropriate formulation strategy for low-solubility drugs with various physical properties.

**Keywords:** Solid amorphous dispersion; HPMCAS; absorption; oral bioavailability; spray drying; solid solution

### Introduction

Low aqueous solubility resulting in poor oral bioavailability of potential drug candidates has been recognized as an increasingly common challenge facing the pharmaceutical industry in the past decade.<sup>1–6</sup> An estimated 25–30% of compounds in early development have poor bioavailability

due to low solubility, representing a significant lost economic and therapeutic opportunity.<sup>7</sup> Because many of these low-solubility compounds have the potential to be safe and efficacious, it is critical that they be developed, even though they may not fit the “rule of five”.<sup>8</sup> The difficulty of designing solubility into a drug candidate while simultaneously retaining potency and selectivity is well-known.<sup>9</sup> Consequently, this situation has provided opportunities to the pharmaceutical scientist as well as drug-delivery technol-

\* To whom correspondence should be addressed. Address: Bend Research Inc., 64550 Research Road, Bend, OR 97701. Telephone: (541) 382-4100. Fax: (541) 382-2713. E-mail: dtfriesen@bendres.com.

† Bend Research Inc.

‡ Pfizer Inc.

§ Current address: Agere Research LLC, Bend, OR 97701.

- (1) Lipinski, C. A. Poor Aqueous Solubility - An Industry Wide Problem in Drug Discovery. *Am. Pharm. Rev.* **2002**, 5, 82–85.
- (2) Lipinski, C. A. Drug-Like Properties and the Causes of Poor Solubility and Poor Permeability. *J. Pharmacol. Toxicol. Methods* **2000**, 44, 235–249.
- (3) Lipinski, C. A. Physicochemical Properties and the Discovery of Orally Active Drugs: Technical and People Issues, Molecular Informatics: Confronting Complexity. In *The Proceedings of the Beilstein-Institut Workshop*; Hicks, M. G.; Kettner, C., Eds.; Beilstein-Institut: Frankfurt, Germany, 2003; May 13–16, 2002, Bozen, Italy.

- (4) Gardner, C. R.; Walsh, C. T.; Almarsson, O. Drugs as Materials: Valuing Physical Form in Drug Discovery. *Nat. Rev. Drug Discovery* **2004**, 3, 926–934.
- (5) Schroter, C. Prioritizing Molecules Based on Physicochemical Characteristics. *Am. Pharm. Rev.* **2006**, 9, 60–67.
- (6) Leuner, C.; Dressman, J. Improving Drug Solubility for Oral Delivery using Solid Dispersions. *Eur. J. Pharm. Biopharm.* **2000**, 50, 47–60.
- (7) Anon., GAO report to Congress, *New Drug Development*, GAO-07-49, November, **2006**.
- (8) Lipinski, C. A.; Lombardo, F.; Dominy, B. W.; Feeney, P. J. Experimental and Computational Approaches To Estimate Solubility and Permeability in Drug Discovery and Development Settings. *Adv. Drug Delivery Rev.* **1997**, 23, 1–3, 3–25.

ogy companies to advance multiple approaches to solubilize such molecules to enhance their oral bioavailability.<sup>10–13</sup>

To address this need, a variety of solubilization techniques have been developed,<sup>14</sup> including those based on the following approaches: (a) formation of salts for ionizable compounds;<sup>15,16</sup> (b) solutions in solvents, cosolvents, and lipids;<sup>17–20</sup> (c) micelle systems, including self-emulsifying drug-delivery systems (SEDDS);<sup>21–26</sup> (d) particle size reduction, including the use of attrition-milled nanocrystalline

forms;<sup>27–32</sup> (e) complexation;<sup>33–35</sup> (f) prodrugs;<sup>36–38</sup> and (g) amorphous solids and solid dispersions.<sup>39–46</sup> Despite the availability of a multitude of solubilization techniques, there

- (9) Ruben, A. J.; Kiso, Y.; Freire, E. Overcoming Roadblocks in Lead Optimization: A Thermodynamic Perspective. *Chem. Biol. Drug Des.* **2006**, *67*, 2–4.
- (10) Anon. *Drug Solubility: Solubilization Technology Platforms and Players*; Applied Data Research: Amherst, NH, March, 2008.
- (11) Hageman, M. Solubility, Solubilization and Dissolution in Drug Delivery During Lead Optimization. In *Optimizing the “Drug Like” Properties of Leads in Drug Discovery, Biotechnology: Pharmaceutical Aspects*; Borchardt, R., Ed.; Springer: New York, 2006; Vol. IV, pp 100–130.
- (12) Timpe, C. Strategies for Formulation Development of Poorly Water Soluble Candidates - A Recent Perspective. *Am. Pharm. Rev.* **2007**, *10*(3), 104–109.
- (13) Chaubal, M. V. Application of Formulation Technologies in Lead Candidate Selection and Optimization. *Drug Discovery Today* **2004**, *9*, 603–609.
- (14) Fahr, A.; Liu, X. Drug Delivery Strategies for Poorly Water-Soluble Drugs. *Expert Opin. Drug Delivery*. **2007**, *4* (4), 403–416.
- (15) Serajuddin, A. T. M. Salt Formation to Improve Drug Solubility. *Adv. Drug Delivery Rev.* **2007**, *59*, 603–616.
- (16) Avdeef, A. Solubility of Sparingly Soluble Ionizable Drugs. *Adv. Drug Delivery Rev.* **2007**, *59*, 568–590.
- (17) Strickley, R. G.; Oliyai, R. Solubilizing Vehicles for Oral Formulation Development. In *Solvent Systems and Their Selection in Pharmaceuticals And Biopharmaceutics, Biotechnology: Pharmaceutical Aspects*; Augustijns, P., Brewster, M. E., Eds.; Springer: New York, 2007; Vol. VI, 257–308.
- (18) Porter, C. J.; Wasan, K. J.; Constantinides, P. Lipid-Based Systems for Enhanced Delivery of Poorly Water Soluble Drugs. *Adv. Drug Delivery Rev.* **2008**, *59*, 615–778 (all papers in this issue).
- (19) Pole, D. L. Physical and Biological Considerations for the Use of Nonaqueous Solvents in Oral Bioavailability Enhancement. *J. Pharm. Sci.* **2008**, *97*, 1071–1088.
- (20) Porter, C. J.; Trevaskis, N.; Charman, W. N. Lipids and Lipid-Based Formulations: Optimizing the Oral Delivery of Lipophilic Drugs. *Nat. Rev. Drug Discovery* **2007**, *6* (3), 231–248.
- (21) Nakano, M. Places of Emulsions in Drug Delivery. *Adv. Drug Delivery Rev.* **2000**, *45*, 1–4.
- (22) Gursoy, R. N.; Benita, S. Self Emulsifying Drug Delivery Systems (SEDDS) for Improved Oral Delivery of Lipophilic Drugs. *Biomed. Pharmacother.* **2004**, *58*, 173–182.
- (23) Gao, P.; Morozowich, W. Development of Supersaturable Self-Emulsifying Drug Delivery System Formulations for Improving Oral Absorption of Poorly Soluble Drugs. *Expert Opin. Drug Delivery*. **2006**, *3*, 97–110.
- (24) Pouton, C. W. Lipid Formulations for Oral Administration of Drugs: Non-Emulsifying, Self-Emulsifying and “Self-Microemulsifying” Drug Delivery Systems. *Eur. J. Pharm. Sci.* **2000**, *11*, S93–S98.
- (25) Gaucher, G.; Dufresne, M.-H.; Sant, V. P.; Kang, N.; Maysinger, D.; Leroux, J. C. Block Copolymer Micelles: Preparation, Characterization and Application in Drug Delivery. *J. Controlled Release* **2005**, *109*, 169–188.
- (26) Rao, V. M.; Nerurkar, M.; Pinnamaneni, S.; Rinaldi, F.; Raghavan, K. Co-Solubilization of Poorly Soluble Drugs by Micellization and Complexation. *Int. J. Pharm.* **2006**, *319*, 98–106.
- (27) Rabinow, B. E. Nanosuspensions in Drug Delivery. *Nat. Rev. Drug Discovery*. **2004**, *3*, 785–796.
- (28) Kesiosoglou, F.; Panmai, S.; Wu, Y. Application of Nanoparticles in Oral Delivery of Immediate Release Formulations. *Curr. Nanosci.* **2007**, *3*, 183–190.
- (29) Bhavsar, M. D.; Shenoy, D. B.; Amji, M. M. *Polymeric Nanoparticles for Delivery in the Gastro-Intestinal Tract. Nanoparticles as Drug Carriers*; Torchilin, V. P., Ed.; Imperial College Press: London, U.K., 2006; pp 609–648.
- (30) Keck, C. M.; Hommoss, A. H.; Mueller, R. H. Lipid Nanoparticles for Encapsulation of Actives: Dermal and Oral Formulations. *Am. Pharm. Rev.* **2007**, *10*, 78–82.
- (31) Merskio-Liversidge, E. M.; Liversidge, G. G. Drug Nanoparticles: Formulating Poorly Water Soluble Compounds. *Toxicol. Pathol.* **2008**, *36*, 43–48.
- (32) Date, A. A.; Patravale, V. B. Current Strategies for Engineering Drug Nanoparticles. *Curr. Opin. Colloid Interface Sci.* **2004**, *9*, 222–235.
- (33) Carrier, R. L.; Miller, L. A.; Ahmed, I. The Utility of Cyclodextrins for Enhancing Oral Bioavailability. *J. Controlled Release* **2007**, *123*, 78–99.
- (34) Brewster, M. E.; Loftsson, T. Cyclodextrins As Pharmaceutical Solubilizers. *Adv. Drug Delivery Rev.* **2007**, *59*, 645–666.
- (35) Davis, M. E.; Brewster, M. E. Cyclodextrin Based Pharmaceutics: Past, Present and Future. *Nat. Rev. Drug Discovery* **2004**, *3*, 1025–1035.
- (36) Rautio, J.; Kumpulainen, H.; Heimbach, T.; Oliyai, R.; Oh, D.; Jarvinen, T.; Savolainen, J. Prodrugs: Design and Clinical Applications. *Nat. Rev. Drug Discovery* **2008**, *7*, 255–270.
- (37) Zentner, G. M.; Delmar, E.; Pleiman, C.; McRea, J. C.; Bajji, A.; Jessing, K.; Mather, G. Formulations and Prodrugs for Delivery of Extremely Insoluble Drugs. *Bull. Tech. Gattefosse* **2003**, *96*, 119–127.
- (38) Chen, H. O.; Schmid, H. L.; Stilgenbauer, L. A.; Howson, W.; Horwell, D. C.; Stewart, B. H. Evaluation of a Targeted Prodrug Strategy To Enhance Oral Absorption of Poorly Water Soluble Compounds. *Pharm. Res.* **1998**, *15*, 1012–1018.
- (39) Vasconcelos, T.; Sarmiento, B.; Costa, P. Solid Dispersions as a Strategy To Improve Oral Bioavailability of Poor Water Soluble Drugs. *Drug Discovery Today* **2007**, *12*, 1068–1075.
- (40) Sethia, S.; Squillante, E. Solid Dispersions: Revival With Greater Possibilities and Applications in Oral Drug Delivery. *Crit. Rev. Drug Carrier Syst.* **2003**, *20*, 215–247.
- (41) Leuner, C.; Dressman, J. Improving Drug Solubility for Oral Delivery Using Solid Dispersions. *Eur. J. Pharm. Biopharm.* **2000**, *50*, 47–60.
- (42) Chokshi, R. J.; Zia, H.; Sandhu, H. K.; Shah, N. H.; Malick, W. A. Improving the Dissolution Rate of Poorly Water Soluble Drugs by Solid Dispersion and Solid Solution—Pros and Cons. *Drug Delivery* **2007**, *14*, 33–45.
- (43) Chawla, G.; Bansal, A. K. A Comparative Assessment of Solubility Advantage From Glassy and Crystalline Forms a Water-Insoluble Drug. *Eur. J. Pharm. Biopharm.* **2007**, *32*, 45–57.
- (44) Shanbhag, A.; Rabel, S.; Nauka, E.; Casadevall, G.; Shivanand, P.; Eichenbaum, G.; Mansky, P. Method for Screening of Solid Dispersion Formulations of Low-Solubility Compounds - Miniaturization and Automation of Solvent Casting and Dissolution Testing. *Int. J. Pharm.* **2008**, *351*, 209–218.

has been a need to identify a robust, reliable, reproducible technology that can be applied broadly to structurally diverse insoluble compounds.

In this paper, we discuss the discovery and development of a spray-dried solid amorphous dispersion technology based on hydroxypropyl methylcellulose acetate succinate (HPMCAS).<sup>47,48</sup> Such “spray-dried dispersions” (SDDs) accomplish the following objectives: (1) enhance the oral absorption of poorly water-soluble compounds by attaining and sustaining a supersaturated concentration of drug in the gastrointestinal (GI) fluid; (2) provide a physically stable drug form (avoiding crystallization or phase separation of amorphous drug) that enables processing of the dispersion into solid dosage forms for shipment and usage; (3) provide a solid drug form that can be manufactured via a reproducible, controllable, and scalable process; and (4) provide a technology that is applicable to structurally diverse insoluble compounds across a wide range of physicochemical properties.

It is well-recognized that the enthalpy, entropy, and free energy of an amorphous solid are higher than those of its crystalline counterpart.<sup>49–53</sup> The excess free energy of an amorphous solid provides a universal method to enhance solubility of structurally diverse organic compounds. However, it is this same excess free energy that provides the driving force for nucleation and crystallization of the drug, making it challenging to use an amorphous drug form in a commercial product.<sup>51–54</sup>

HPMCAS-based SDDs were developed to take advantage of the positive attributes of amorphous drug forms while overcoming their associated challenges. We have also used a spray-drying process that offers a reproducible method for forming dispersions that is applicable to drugs with a wide range of physicochemical properties.

- (45) Vandecruys, R.; Peeters, J.; Verreck, G.; Brewster, M. E. Use of a Screening Method To Determine Excipients Which Optimize the Extent and Stability of Supersaturated Drug Solutions and Application of This System to Solid Formulation Design. *Int. J. Pharm.* **2007**, *342*, 168–175.
- (46) Kaushal, A. M.; Gupta, P.; Bansal, A. K. Amorphous Drug Delivery Systems: Molecular Aspects, Design and Performance. *Crit. Rev. Ther. Drug Carrier Syst.* **2004**, *21*, 133–193.
- (47) Curatolo, W. J.; Herbig, S. M.; Nightingale, J. A. S. Solid Pharmaceutical Dispersions with Enhanced Bioavailability. European Patent Application EP 0 901 786 A2, 1999.
- (48) HPMCAS is also known as hypromellose acetate succinate.
- (49) Kauzmann, W. The Nature of Glassy State and the Behavior of Liquids at Low Temperatures. *Chem. Rev.* **1948**, *43*, 219–256.
- (50) Davies, R. O.; Jones, G. O. Thermodynamic and Kinetic Properties of Glasses. *Adv. Phys.* **1953**, *2*, 370–410.
- (51) Gutzow, I.; Schmelzer, J. *The Vitreous State: Thermodynamics, Structure, Rheology and Crystallization*; Springer, Heidelberg, Germany, 1995.
- (52) Donth, E. *The Glass Transition: Relaxation Dynamics in Liquids and Disordered Materials*; Springer, Berlin, Germany, 2001.
- (53) Schmelzer, J. W. P. Crystal Nucleation and Growth in Glass Forming Melts: Experiment and Theory. *J. Non-Cryst. Solids* **2008**, *354*, 269–278.
- (54) Bhugra, C.; Pikal, M. J. Role of Thermodynamic, Molecular and Kinetic Factors in Crystallization from the Amorphous State. *J. Pharm. Sci.* **2008**, *97*, 1329–1349.

The purpose of this paper is to provide an overview of the key features of the SDD solubilization technology. In the following sections, we describe (1) the unique features of HPMCAS that make it ideal for use in forming homogeneous solid amorphous dispersions of a low-solubility drug; (2) the spray-drying process used to form homogeneous SDDs; (3) the solid-state properties of the SDDs that provide kinetic stability of the dispersions; (4) the species that form when SDDs are dosed to *in vitro* or *in vivo* aqueous solutions, which lead to enhanced oral absorption relative to crystalline drug; and (5) the broad applicability of this technology for drugs with a wide range of physicochemical properties. Future publications will focus on the scientific details of the mechanism of *in vivo* absorption, manufacturing, and physical stability.

## Experimental Section

**Materials.** HPMCAS (AQOAT) was purchased from Shin-Etsu Chemical Co., Ltd. (Tokyo, Japan). Several grades of HPMCAS are available. The manufacturer reports that the respective grades are soluble in McIlvaine’s buffer solution at the following pH values: -LF and -LG,  $\geq 5.5$ ; -MF and -MG,  $\geq 6.0$ ; and -HF and -HG,  $\geq 6.8$ .<sup>55</sup> However, we have found that the -LF and -LG grades are sparingly soluble, dispersing to form colloidal solutions in aqueous solutions at pH > about 4.8, the -MF and -MG grades at pH > about 5.2, and -HF and -HG grades at pH > about 5.7.

Other polymers tested were hypromellose (also known as hydroxypropyl methylcellulose, or HPMC), purchased as Methocel E3 Premium LV from Dow Chemical Co. (Midland, MI), and Povidone K12 [also known as polyvinyl pyrrolidone (PVP)], purchased from International Specialty Products (Wayne, NJ).

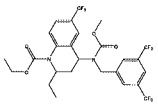
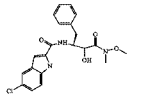
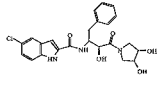
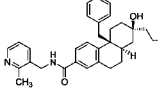
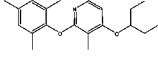
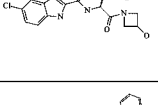
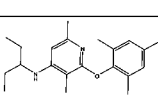
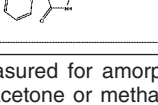
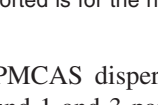
The drugs and drug candidates studied are presented in Table 1.<sup>56</sup> All were provided by Pfizer Global Research and Development. The physical properties of these compounds, determined in the authors’ laboratories, are also presented in Table 1. The  $c \log P$  values were calculated using a temperature of 25 °C. The glass-transition temperatures ( $T_g$ ’s) and melting temperatures ( $T_m$ ’s) were determined at an accuracy of  $\pm 2$  °C using differential scanning calorimetry (DSC) analysis, as described below. Samples of each compound were equilibrated at a relative humidity (RH) of less than 5% overnight prior to DSC analysis. Aqueous solubilities were determined at 37 °C by measuring the concentration of the lowest-energy crystalline form of the compound (for basic compounds, the free-base form was used) in a pH 6.5 phosphate buffered saline (PBS) solution (described in the Dissolution Testing section) using high-performance liquid chromatography (HPLC) analysis, except for Compounds 1, 4, and 7 (see the description below).

SDD composition is reported in terms of the weight percent (wt %) drug in the dispersion. For example, a 25-wt %

(55) Shin-Etsu Chemical Co. Ltd. (Tokyo, Japan) product literature on AQOAT.

(56) Throughout this paper, drug candidates are referred to as drugs or by a compound number.

**Table 1.** Structure and Properties of Compounds Studied

Compound	Structure	Name	$c \log P$	$T_g$ (°C)*	$T_m$ (°C)	Aqueous Solubility of Crystalline Compound (µg/mL)**	pK <sub>a</sub>
Compound 1		[2 <i>R</i> ,4 <i>S</i> ]-4-[(3,5-Bis-trifluoromethyl-benzyl)-methoxycarbonyl-amino]-2-ethyl-6-trifluoromethyl-3,4-dihydro-2H-quinoline-1-carboxylic acid ethyl ester (also known as torcetrapib)	6.7	29	90	<0.1	None
Compound 2		[ <i>R</i> -( <i>R</i> *, <i>S</i> *)]-5-Chloro- <i>N</i> -{2-hydroxy-3-[(methoxymethyl-amino)-3-oxo-1-(phenylmethyl)propyl]propyl}-1H-indole-2-carboxamide	3.9	87	192	1	None
Compound 3		5-Chloro-1H-indole-2-carboxylic acid {(1 <i>S</i> )-benzyl-(2 <i>R</i> )-hydroxy-3-[(3 <i>R</i> ,4 <i>S</i> )-dihydroxy-pyrrolidin-1-yl]-3-oxypropyl} amide	3.1	96	238	80	8.5, 12.9
Compound 4		2-Phenanthrenecarboxamide, 4b, 5, 6, 7, 8, 8a, 9, 10-octahydro-7-hydroxy- <i>N</i> -[(2-methyl-3-pyridinyl)methyl]-4b-(phenylmethyl)-7-(3,3,3-trifluoropropyl)-, (4b <i>S</i> ,7 <i>S</i> ,8a <i>R</i> )	6.24	99	225	0.0038	None
Compound 5		3,6-Dimethyl-4-(3-pentoxo)-2-(2,4,6-trimethylphenoxy)pyridine	6.76	-27	76	< 0.2	3.5
Compound 6		5-Chloro-1H-indole-2-carboxylic acid [(1)-benzyl-2-(3-hydroxy-azetidin-1-yl)-2-oxo-ethyl]-amide	4.06	92	175	14.6	None
Compound 7		5-[2-[4-(Benzo[d]isothiazol-3-yl)piperazin-1-yl]ethyl]-6-chloroindolin-2-one	3.6	173	304	0.1	6.5, 10
Compound 8		[3,6-Dimethyl-2-(2,4,6-trimethyl-phenoxy)-pyridin-4-yl]-(1-ethyl-propyl)-amine	6.3	87	224	0.03	6.9
Compound 9		5,5-Diphenyl-2,4-imidazolidinedione	2.47	71	299	26	8.3

\*  $T_g$ 's were measured for amorphous samples of the compound prepared by spray-drying from a solution of the compound in organic solvent (typically acetone or methanol) using a process similar to that used to prepare SDDs (see Spray-Drying Process for Making SDDs section). All samples were shown to be at least 95% amorphous by the lack of sharp diffraction lines in their PXRD patterns. \*\* Solubility of the lowest-energy crystalline form in pH 6.5 PBS solution measured at 37 °C. For basic compounds, the free-base form was used and the solubility value reported is for the neutral (that is, un-ionized) form of the compound.

Compound 1/HPMCAS dispersion consists of 1 part (by weight) Compound 1 and 3 parts (by weight) HPMCAS.

Solvents and chemicals used to prepare spray-drying solutions and perform *in vitro* tests were purchased from Sigma-Aldrich Co. (Milwaukee, WI) or similar sources, except for 1-palmitoyl-2-oleyl-*sn*-glycero-3-phosphocholine

(POPC), which was purchased from Avanti Polar Lipids Inc. (Alabaster, AL).

PBS used in dissolution tests consisted of 20 mM sodium phosphate (Na<sub>2</sub>HPO<sub>4</sub>), 47 mM potassium phosphate (KH<sub>2</sub>PO<sub>4</sub>), 87 mM sodium chloride (NaCl), and 0.2 mM potassium chloride (KCl), adjusted to pH 6.5 with sodium



hydroxide (NaOH), with an osmolarity of 290 mOsm/kg. Model fasted duodenal (MFD) solution was PBS solution containing 7.3 mM sodium taurocholic acid (NaTC) and 1.4 mM POPC. The taurocholate and phosphocholine compounds form mixed micelles and mimic those present in the GI tract, solubilizing hydrophobic compounds. A “2% MFD” solution was also used, which consisted of the PBS solution containing 29.2 mM NaTC and 5.6 mM POPC. The 2% MFD solution was used to determine the dissolution of drug forms in solutions that have a high level of mixed micelles, as might be present in the small intestine following ingestion of a meal.

**Methods. DSC Analysis.** Amorphous samples of the compound were prepared by spray-drying from a solution of the compound in acetone or methanol using a process similar to that used to prepare SDDs (see Spray-Drying Process for Making SDDs section). DSC analyses were performed using a Thermal Analysis Q1000 differential scanning calorimeter equipped with an autosampler. Sample pans were equilibrated at the desired RH overnight, crimped and sealed, and then loaded into the differential scanning calorimeter. The samples were heated by modulating the temperature (for example, at  $\pm 1.5$  °C/min) while increasing the temperature at a rate of 2.5 °C/min.

**Powder X-Ray Diffraction (PXRD) Analysis.** Samples were examined using PXRD with a Bruker AXS D8 Advance diffractometer. Samples (approximately 100 mg) were packed in 0.5-mm-deep zero-background-holder sample cups. Samples were spun in the  $\varphi$  plane at 30 rpm to minimize crystal orientation effects. The X-ray source (KCu $\alpha$ ,  $\lambda = 1.54$  Å) was operated at 45 kV and 40 mA. Data for each sample were collected from 4° to 40° on the  $2\theta$  scale over 30 min in continuous detector scan mode at a scan speed of 2 s/step and a step size of 0.04°/step.

**Dynamic Vapor Sorption (DVS).** DVS experiments were used to determine the water uptake of polymers at 25 °C as a function of RH using a TA Q5000 TGA instrument (TA Instruments, New Castle, DE). Samples of about 5–25 mg were analyzed with a humidity step size of 10%. Samples were assumed to be at equilibrium when the change in mass was less than 0.0002 mg/min.

**Scanning Electron Microscopy (SEM).** SEM was used to obtain particle size and morphology information about the SDDs using a Hitachi S-3400N microscope. Samples were sputtered with gold/palladium to provide a conductive coating.

**Solubility Testing.** Solubility was measured (except for Compounds 1, 4, and 7) by adding an excess of crystalline drug to PBS solution at 37 °C. The suspension was agitated. The suspension remained at 37 °C for at least 1 h and then was centrifuged, and the concentration of the supernatant was measured by HPLC. For Compounds 1 and 4, which have extremely low solubility, solubility was estimated by first measuring the solubility of the amorphous form of the compound as described above (that is, add excess, agitate, centrifuge, and analyze by HPLC) in PBS solutions containing various concentrations of micelles (NaTC/POPC) and

extrapolating to zero-concentration micelles. The crystalline solubility was then calculated by dividing the amorphous solubility by the ratio of the NMR-visible drug for crystalline drug using 2% MFD solution as the medium. For Compound 7, the solubility of the free-base crystalline form was measured as a function of pH and the solubility of the neutral form was estimated by fitting the data to the Henderson–Hasselbalch equation.<sup>57</sup>

**Dissolution Testing.** The following *in vitro* dissolution test was performed on SDDs and crystalline or amorphous drug to determine the concentration enhancement relative to the bulk crystalline or amorphous form of the drug. A sufficient amount of material was added to a microcentrifuge test tube to achieve the desired dose if all the drug dissolved. The tubes were placed in a 37 °C temperature-controlled chamber, and 1.8 mL of PBS or MFD solution was added to each tube. The samples were quickly mixed using a vortex mixer for about 60 s. At each time point, the samples were centrifuged at 13 000g at 37 °C for 1 min. The supernatant solution was sampled and diluted 1:6 (by volume) with methanol and then analyzed by HPLC. Following sampling, the contents of each tube were mixed on the vortex mixer for about 60 s and then allowed to stand undisturbed at 37 °C until the next sample was taken.

**Cryogenic Transmission Electron Microscopy (TEM).** Samples from a dissolution test (see Dissolution Testing section) were frozen in liquid ethane onto a carbon TEM grid and kept frozen under liquid nitrogen until imaging. The frozen sample was imaged in an FEI Tecnai20 Sphera TEM at 200 kV.

**Dynamic Light Scattering.** The solid dispersion was added to PBS and equilibrated to 37 °C for 2 h. After 2 h, 2 mL of solution was removed and centrifuged at 13 000g for 1 min to remove precipitated material, leaving free drug, free polymer, and drug/polymer assemblies in solution. Dynamic light scattering (based on diffusion of particles) of the supernatant of each of the centrifuged solutions was measured using a PSS NICOMP 380 submicron particle sizer, and the size of drug and polymer particles in the solution was calculated.

**Nuclear Magnetic Resonance (NMR) Determination of Free Drug.** For compounds containing a fluorine atom, the drug was dosed into PBS containing a specific concentration of NaTC and POPC. An internal standard, trifluoroacetic acid (TFA), was also added. The sample temperature was maintained at 37 °C in the probe. Spectra were collected overnight. Fluorine <sup>19</sup>NMR spectra were recorded at 282.327 MHz on a Varian 300-MHz NMR instrument equipped with a Nalorac 8-mm indirect detection probe. Drug resonances were integrated relative to the internal standard peak. NMR-visible drug concentrations were determined from the ratio of the measured peak area to the peak area for an organic solution of the same drug of known concentration. For compounds that do not have

(57) Hendricksen, B. A.; Sanchez, F. M. V.; Bolger, M. B. The Composite Solubility Versus pH Profile and Its Role in Intestinal Absorption Prediction. *AAPS Pharm. Sci.* **2003**, *5*, 1–15, Article 4.

a fluorine atom, proton NMR was used. The measurement method was similar to the fluorine NMR method described above, but measurements were performed on a Bruker 500-MHz NMR instrument using trimethylsilyl-2,2,3,3-tetradeuteriopropionic acid sodium salt (TSP) as an internal standard.

**In Vivo Dosage Form Preparation and Testing.** SDDs were constituted into oral powder for constitution (OPC) formulations by adding water and agitating. Alternatively, the SDD was filled into a gelatin capsule.

Relative bioavailability was tested *in vivo* using conventional methods. *In vivo* tests were performed in dogs using the following general procedure. The SDD was dosed orally to a group of fed or fasted beagle dogs, and drug release was monitored by periodically withdrawing blood and measuring the plasma drug concentration. The area under the concentration-versus-time curve (AUC) was determined from the time the dose was administered to the last sample. Crystalline drug alone was tested as a control. The crystalline drug was administered as an aqueous suspension in a solution containing 0.5-wt % Methocel (USP grade, 4000 cps, Dow Chemical Co.). The SDD OPC formulation or crystalline drug suspension was dosed orally using an oral gavage equipped with a polyethylene tube insert. The polyethylene tube insert was used to accurately deliver the desired volume of dose by displacement, without the need for an additional volume of water to rinse the tube.

Whole-blood samples (3-mL red-top Vacutainer tubes without serum separators) were taken from the jugular or cephalic vein before dosing and at various time points after dosing. Serum was harvested into tubes containing potassium ethylenediaminetetraacetic acid (K<sub>2</sub>EDTA) anticoagulant. Blood was maintained on wet ice prior to centrifugation to obtain plasma. Centrifugation, which began within 1 h of collection, was performed at 2500 rpm for 15 min. Plasma was maintained on dry ice prior to storage at approximately -70 °C. Plasma was analyzed using standard liquid chromatography techniques.

*In vivo* tests in humans used the following general procedure. The SDD was dosed as an OPC to healthy humans ( $n = 3$  or 4) who had fasted overnight, whereas crystalline drug was dosed as an OPC or in a gelatin capsule. Drug concentration in the blood plasma was determined periodically by withdrawing blood and measuring the plasma drug concentration using liquid chromatography/mass spectroscopy techniques.

## Results and Discussion

An SDD is a single-phase, amorphous molecular dispersion of a drug in a polymer matrix. It is a solid solution with the compound molecularly dissolved in a solid matrix.<sup>58</sup> As the name suggests, SDDs are obtained by dissolving drug and polymer in a solvent (typically acetone or methanol) and

then spray-drying the solution. Process conditions are chosen so that the solvent rapidly evaporates from the droplets to rapidly solidify the polymer and drug mixture, trapping the drug in amorphous form as an amorphous molecular dispersion. As described below, by using HPMCAS as the solid matrix, these homogeneous (that is, single-phase) SDDs are physically stable, allowing for long-term storage over a wide range of conditions without amorphous phase separation or crystallization of the drug.

The drug in an SDD is in a high-energy state relative to crystalline drug. When placed into an aqueous solution, SDDs dissolve to a concentration of drug well above the solubility of its lowest-solubility crystalline form. This higher concentration provides the driving force for rapid absorption of the drug.

**HPMCAS.** The choice of polymer from which the SDD is made is critical. HPMCAS has unique properties that make it ideal for use in SDDs, including the following.

(1) It has a high  $T_g$  in its un-ionized state. This high  $T_g$  directly correlates to the drug having low mobility, which is responsible for the excellent physical stability of HPMCAS SDDs.

(2) It is highly soluble in volatile organic solvents, such as acetone and methanol, allowing for economical and controllable processes for forming SDDs.

(3) When at least partially ionized, as it is at any pH above about 5, the charge on the polymer minimizes formation of large polymer aggregates, allowing drug/polymer colloids (for example, amorphous nanostructures) to remain stable.

(4) The amphiphilic nature of HPMCAS allows insoluble drug molecules to interact with the hydrophobic regions of the polymer, whereas the hydrophilic regions allow these structures to remain as stable colloids in aqueous solution.

HPMCAS is a cellulosic polymer with four types of substituents semirandomly substituted on the hydroxyls: methoxy, with a mass content of 12–28 wt %; hydroxypropyl, with a mass content of 4–23 wt %; acetate, with a mass content of 2–16 wt %; and succinate, with a mass content of 4–28 wt %.<sup>59</sup> The succinate groups of HPMCAS have a  $pK_a$  of about 5, and therefore, the polymer is less than 10% ionized at pH values below about 4 and is at least 50% ionized at pH values of about 5 or higher.<sup>60</sup> Due to the presence of relatively hydrophobic methoxy and acetate substituents, HPMCAS is water-insoluble when un-ionized (about pH < 5) and remains predominantly colloidal at intestinal pH (that is, pH 6.0–7.5).

In its un-ionized state (as it is in the solid SDD before dissolution), HPMCAS has a high  $T_g$ , even when exposed to high RH. Figure 1a shows the  $T_g$  versus the RH of air to which the samples were equilibrated<sup>61</sup> for the three com-

(58) The compound concentration in the HPMCAS matrix may be above its thermodynamically stable value as long as the low mobility of the compound inhibits its ability to migrate, phase separate, and, ultimately, crystallize. This physical stability property is related to the high  $T_g$  of the glassy dispersion relative to normal storage temperatures. This is discussed in the section titled Solid-State Properties.

(59) Official Monograph for Hypromellose Acetate Succinate. National Formulary (NF) 25, 2006, 1136–1138.

(60) There are three commercial grades of HPMCAS. The approximate pH values above which each grade becomes aqueous dispersible or soluble are -H grade, 5.7; -M grade, 5.2; and -L grade, 4.8.

(61) Polymer and SDD samples were equilibrated to humidified air at the specified RH at ambient temperature (about 22 °C).

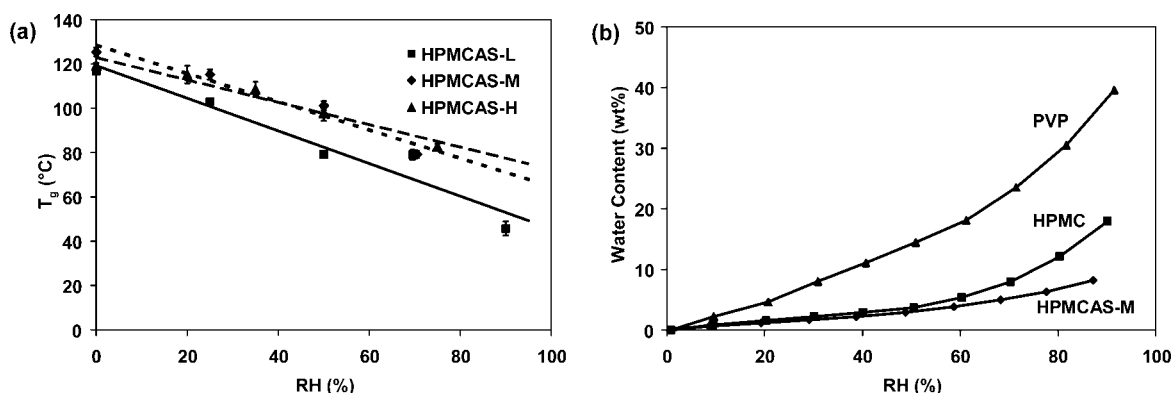


**Figure 1.** Effect of RH on polymer properties: (a)  $T_g$  versus the RH to which samples were equilibrated (at ambient temperature) for HPMCAS and (b) equilibrium water absorption versus RH for HPMCAS, PVP, and HPMC (measured at 25 °C).

mercially available grades of HPMCAS.<sup>62</sup> Under dry conditions, the  $T_g$  is on the order of 120 °C. Like all amorphous materials, when exposed to humid air, HPMCAS absorbs water, which plasticizes the polymer, increasing its mobility. This is reflected in a decrease in its  $T_g$ . However, the relative hydrophobicity of HPMCAS results in much less absorption of water than is observed for typical water-soluble polymers. As shown in Figure 1b, at 75% RH, PVP and HPMC absorb approximately 23 and 10 wt % water respectively, whereas HPMCAS-M absorbs only about 6 wt % water. As a result, the  $T_g$  value of HPMCAS remains above about 70 °C, even when equilibrated with 75% RH air. The low mobility of drug molecules dispersed in such high- $T_g$  glassy polymers leads to the excellent physical stability observed for HPMCAS-based SDDs.

SDDs are formed using HPMCAS in its un-ionized (protonated) form. In this form, it is quite soluble in volatile organic solvents such as methanol and acetone. Since many drug candidates are soluble in these solvents, drug candidates can be processed into HPMCAS-based dispersions readily and economically using a spray-drying process.

HPMCAS contains many substituents that are quite hydrophobic. As a result, even when HPMCAS becomes ionized, as it does at the pH in the small intestine, the polymer is still only sparingly soluble and exists as colloidal polymer aggregates in aqueous solutions.

The colloidal nature of HPMCAS when ionized, combined with the hydrophobic nature of the substituents on the polymer, allows insoluble drug molecules to interact with the polymer, leading to the formation of amorphous drug/polymer nanostructures in solution. The negative charge of the ionized succinate groups keeps these nanostructures stable, avoiding large hydrophobic aggregates of the polymer and drug in solution. These drug/polymer nanostructures constitute a high-energy (high-solubility) form of amorphous drug that is quite stable—often for several hours, or even days—in aqueous suspensions. *In vitro* measurements have shown that drug in these nanostructures can rapidly dissolve to a high free-drug concentration that is supersaturated

relative to crystalline drug. Based on these *in vitro* observations, it is believed that *in vivo*, as drug partitions into bile-salt micelles and is absorbed from the intestine and into systemic circulation, drug can rapidly dissolve from these nanostructures to replace this drug and thereby maintain a supersaturated free-drug concentration. These properties ultimately lead to the enhanced absorption observed when HPMCAS-based SDDs are dosed orally.

**Spray-Drying Process for Making SDDs.** Spray-drying is a well-established and widely used industrial process for transforming solutions, emulsions, or suspensions of materials into dry powdered forms.<sup>63</sup> This transformation is accomplished by pumping a feed solution (for example, drug and HPMCAS dissolved in a volatile solvent) to an atomizer inside a drying chamber. The atomizer breaks the solution up into a plume of small droplets (typically less than 100  $\mu\text{m}$  in diameter). In the drying chamber, the droplets are mixed with a hot drying-gas stream (typically nitrogen). Heat is transferred from the hot drying gas to the droplets to provide the latent heat of vaporization required for rapid evaporation of the solvent from the droplets. As the solvent is removed from the droplet, a high-viscosity gel or “skin” forms on the outside of the droplet, due to the film-forming properties of HPMCAS. Typically, at this stage of drying, the skin is sufficiently flowable (due to the high solvent-to-solids ratio) that the particle skin collapses on itself as the solvent evaporates from the core, yielding particles with the shape shown in Figure 2. By controlling the temperature at the inlet and outlet of the spray dryer, along with the rate at which spray solution and drying gas are introduced to the spray dryer, the morphology, particle size, and density of the resulting SDD powder can be controlled. The solid powder is typically collected from the gas stream using a cyclone or filter system.

Spray-drying under the proper conditions (sufficiently high drying-gas inlet temperature and sufficiently high ratio of gas flow to liquid flow) results in the rapid removal of solvent from the droplets of the spray solution. This, in turn, results

(62) Available from Shin-Etsu Chemical Co. Ltd. (Tokyo, Japan).

(63) Masters, K. *Spray Drying Handbook*, 4th ed.; Halstead Press: New York, 1985.



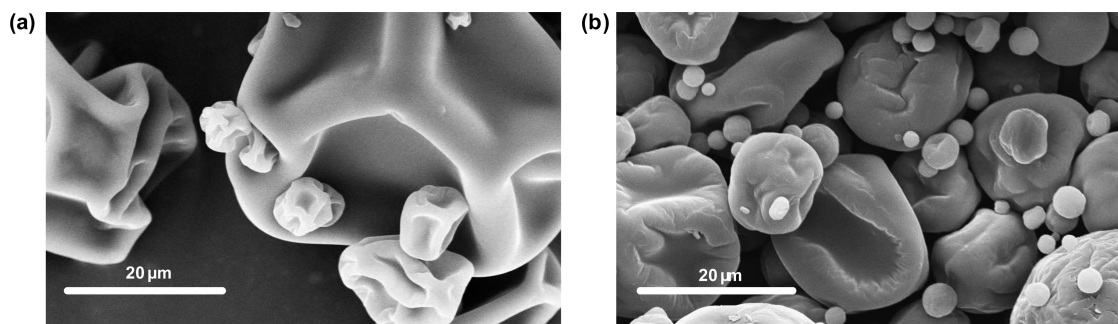


**Figure 2.** SEM images for (a) 25-wt % Compound 1/HPMCAS-M SDD and (b) 67-wt % Compound 2/HPMCAS-M SDD. Images captured at 1500 $\times$  magnification. The bar in each image corresponds to 20  $\mu\text{m}$ .

in rapid solidification of the droplets, which is necessary to prevent phase separation of the drug from the HPMCAS. In addition, the spray-drying process can be performed at a wide range of scales, from small-scale production for initial feasibility studies (milligrams or grams of drug) to full-scale commercial production (tons of drug). During initial formulation work, recovery of active as SDD is typically 70–90% at the gram scale. During clinical-supply manufacture, recovery of active as SDD is typically 80–95% at the kilogram scale. Finally, the spray-drying process can be tuned to produce particles with properties amenable to further processing to form solid oral dosage forms such as tablets or capsules.

**Solid-State Properties.** Selection of the right solvent and spray-drying conditions results in the formation of a homogeneous solid amorphous SDD. PXRD can be used to quantify the presence of crystalline material in SDDs to about 5% or less, depending on the crystal size and shape.<sup>64,65</sup> As an example, Figure 3 compares the PXRD patterns for crystalline material and SDDs for four example compounds. The broad, featureless scattering profiles for the SDDs are strong evidence that more than 95 wt % of the drug in the SDD is amorphous.

PXRD analysis shows that the SDDs do not contain crystalline drug, but it does not reveal that the SDD is homogeneous, containing a solid solution of drug and HPMCAS. For this characterization, DSC is used. DSC has been used extensively in the polymer industry to determine the extent of mixing in polymer systems.<sup>66</sup> A physical mixture of amorphous drug particles and polymer particles will exhibit two distinct  $T_g$  values when analyzed by DSC: one for the drug and one for the polymer. This is shown in Figure 4, which shows the DSC analysis of amorphous drug alone ( $T_g$  of 29 °C), polymer alone ( $T_g$  of 119 °C), and a

physical mixture of amorphous drug and polymer. As shown, the physical mixture shows two  $T_g$  values at 29 and 116 °C, corresponding to the drug and polymer, respectively.

In an SDD, the amorphous drug is molecularly dispersed in the HPMCAS. As a result, the SDD exhibits a single  $T_g$  that is intermediate between that of the pure amorphous drug and pure polymer. As shown in Figure 4, the  $T_g$  for the SDD is 82 °C. This indicates that the SDD is homogeneous, with the drug and polymer forming a drug/polymer phase that has different properties from those of pure amorphous drug or pure polymer.

Using experimental data and calculations based on Flory–Huggins theory,<sup>67</sup> the binary phase diagram was calculated for amorphous Compound 1 and HPMCAS-M, defining the boundary between the one-phase and two-phase regions (that is, the binodal curve).<sup>68</sup> In short, the equilibrium solubility of amorphous Compound 1 in HPMCAS was measured at several different temperatures. Homogeneous dispersions with drug loadings varying from 10 to 50 wt % were formed by spray-drying and then heated to the temperature of interest and held at that temperature until the material no longer changed composition. That is, for dispersions in which the concentration of Compound 1 was below its solubility at the given temperature, the dispersion remained homogeneous. For dispersions above the solubility, a pure amorphous Compound 1 phase would form and grow in volume until the Compound 1/HPMCAS phase reached the equilibrium solubility of Compound 1 in HPMCAS at that temperature. This procedure worked well above 80 °C because (1) the time to equilibrium was relatively fast and (2) no crystallization of the pure Compound 1 phase occurred, since the  $T_m$  of Compound 1 is about 90 °C. In this way, the solubility of Compound 1 in HPMCAS versus temperature was determined between 80 and 120 °C. These data were used to determine  $X$ , the Flory–Huggins parameter for the interaction of Drug 1 and HPMCAS. When used in the Flory–Huggins equation, a value of  $X = 456 \text{ K}^{-1}$  yields the best fit to the solubility-versus-temperature data (that is, the “binodal curve”).<sup>67</sup>

(64) Clas, S.; Faizer, R.; O'Connor, R.; Vadas, E. Quantification of Crystallinity in Blends of Lyophilized and Crystalline MK-0591 using X-Ray Powder Diffraction. *Int. J. Pharm.* **1995**, *121*, 73–79.

(65) de Villiers, M.; Wurster, D.; Van der Watt, J.; Ketkar, A. X-Ray Powder Diffraction Determination of the Relative Amount of Crystalline Acetaminophen in Solid Dispersions With Polyvinylpyrrolidone. *Int. J. Pharm.* **1998**, *163*, 219–224.

(66) Utracki, L. *Polymer Alloys and Blends: Thermodynamics and Rheology*; Hanser Publishers: Munich, Germany, 1989.

(67) Strobl, G. R. *The Physics of Polymers*, 2nd ed.; Springer Verlag: Berlin, Germany, 1997; pp 83–100.

(68) Details of these calculations are beyond the scope of this overview paper and will be presented elsewhere.



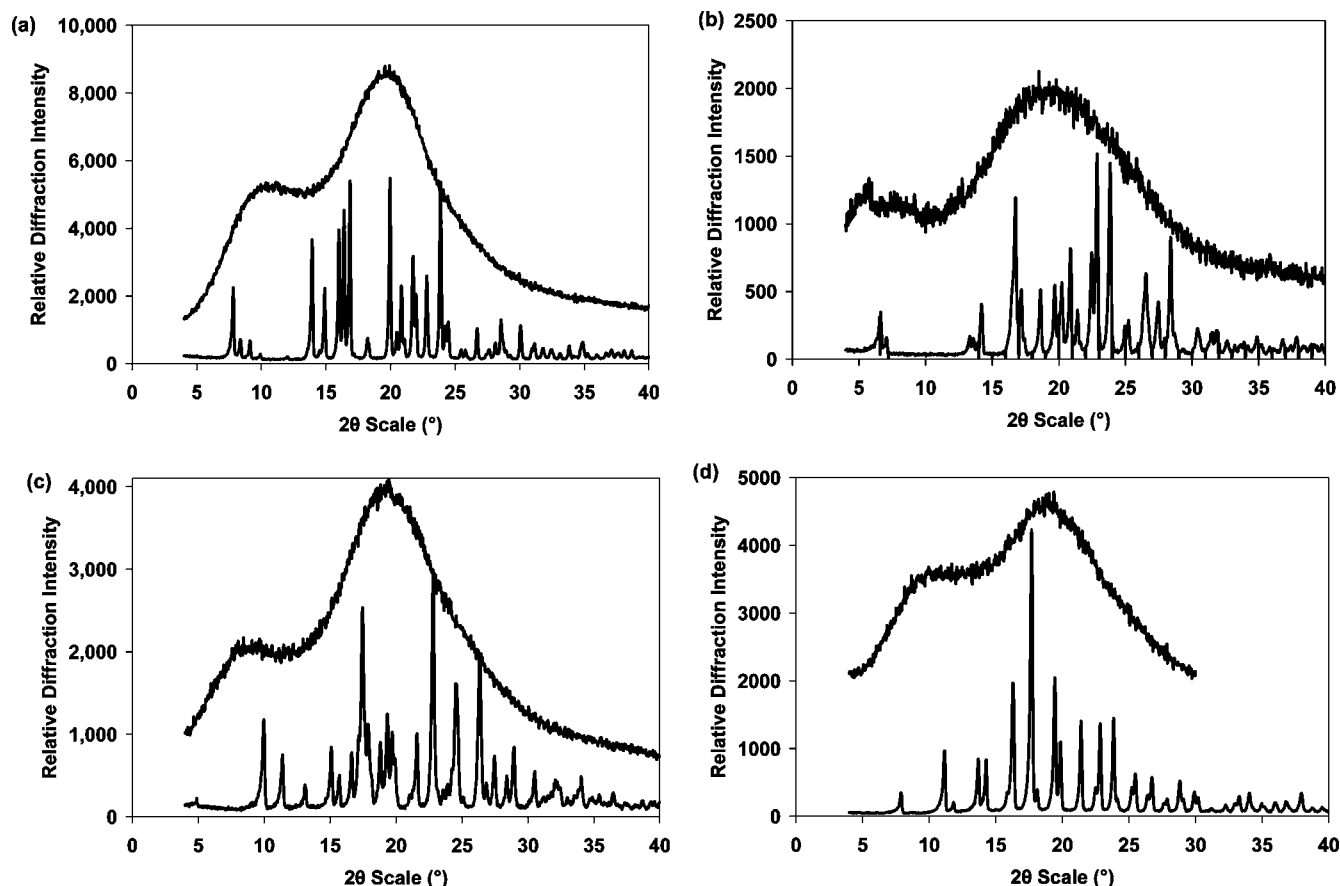


**Figure 3.** PXRD patterns comparing crystalline drug alone with the corresponding SDD for (a) 25-wt % Compound 1/ HPMCAS-M SDD, (b) 67-wt % Compound 2/HPMCAS-M SDD, (c) 50-wt % Compound 3/HPMCAS-M SDD, and (d) 25-wt % Compound 4/HPMCAS-M.

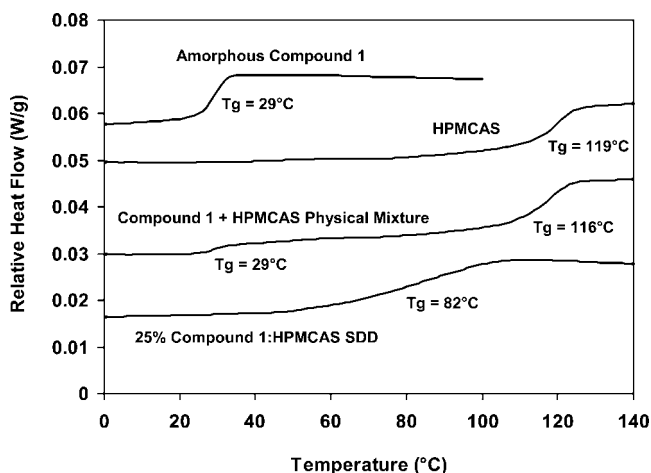


**Figure 4.** DSC data for amorphous Compound 1 alone, HPMCAS alone, a physical mixture of Compound 1 and HPMCAS, and a 25-wt % Compound 1/HPMCAS SDD. Samples were equilibrated at <5% RH prior to analysis. The presence of a single  $T_g$  intermediate to the  $T_g$  values of Compound 1 and HPMCAS indicates that the SDD is a homogeneous solid solution of the compound in the polymer.

Flory–Huggins theory was used to calculate the remainder of the binodal curve (outside the range for which we were able to collect data) as well as the spinodal curve—the curve

separating the two-phase metastable and two-phase unstable regions—using this value of  $X$  and the molar volumes of Compound 1 ( $\nu_{\text{Compound 1}} = 466 \text{ cm}^3/\text{mol}$ ) and HPMCAS ( $\nu_{\text{HPMCAS}} = 42,000 \text{ cm}^3/\text{mol}$ ). These results, which are presented in the phase diagram in Figure 5, indicate that amorphous Compound 1 has a solubility in HPMCAS of about 15–18 wt % between 0 and 50 °C (the pharmaceutically relevant temperature range). In addition, the phase diagram in Figure 5 suggests that, between 0 and 50 °C, a dispersion of amorphous drug and HPMCAS containing 25-wt % drug is in the two-phase metastable region. In the two-phase metastable region, a drug concentration of 25 wt % is slightly supersaturated (supersaturation ratio of 1.4 to 1.7). For dispersions in the two-phase metastable region, the driving force for phase separation is low and there exists a significant energy barrier for drug and polymer to diffusively phase separate.<sup>69</sup> As a result, dispersions in the region phase separate via the nucleation of a pure amorphous drug phase of sufficient size to be “stable” (that is, the derivative of

(69) By “diffusive energy barrier” is meant that the value of  $G_{C+\delta} + G_{C-\delta} - 2G_C$  calculated for  $C = 0.25$  weight fraction is positive, where  $G_C$  is the free energy at weight fraction,  $C$ , of drug in the SDD, and  $\delta$  is a small concentration perturbation. The value is negative in the two-phase unstable region. See Strobl, G.R. *The Physics of Polymers*, 2nd ed.; Springer Verlag: Berlin, Germany, 1997; pp 100–106.

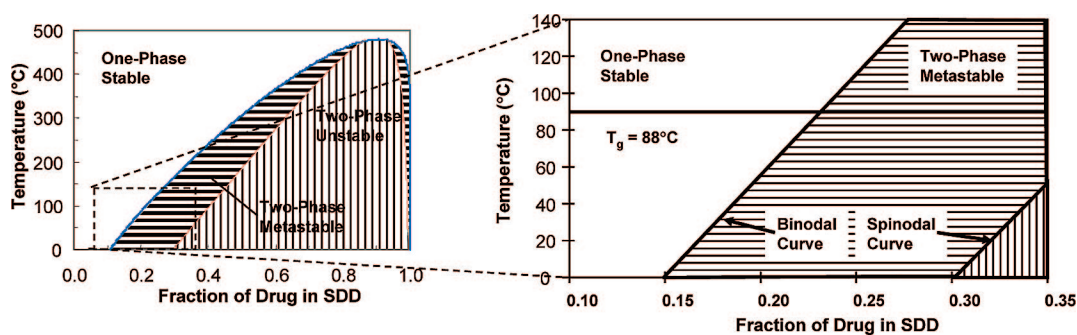


**Figure 5.** Phase diagram of Compound 1 in HPMCAS-M, showing temperature as a function of the weight fraction of drug in the SDD. The calculated binodal curve represents the boundary between the one-phase and two-phase regions, and the calculated spinodal curve represents the boundary between the two-phase metastable and two-phase unstable regions.

free energy with respect to domain size is negative) followed by growth of the domain size (that is, nucleation and growth). In contrast, for dispersions that lie in the two-phase unstable region, there is no diffusive energy barrier and such dispersions phase separate via spinodal decomposition. We have found that dispersions of Compound 1 in HPMCAS that lie in the metastable region show no tendency to phase separate for long storage times.<sup>70</sup> For example, a 25-wt % Compound 1/HPMCAS-M SDD shows no indication of phase separation when stored for 36 months at 25 °C and 60% RH or when stored for 6 months at 40 °C and 75% RH. In conclusion, the first reason for the high stability of HPMCAS-based SDDs is the high solubility of most compounds in HPMCAS.

The second reason for the high stability of HPMCAS-based SDDs is their high  $T_g$  values, which are due to the high  $T_g$  of the polymer. Figure 6 shows the  $T_g$  as a function of the RH of air to which the SDD was equilibrated (at ambient temperature, about 22 °C) for a 25-wt % Compound 1/HPMCAS-M SDD. This shows that the  $T_g$  of the SDD is very high, well above the typical storage temperatures for RH values up to about 50–60%. As a result, the mobility of the drug in the SDD (that is, the diffusion coefficient of drug in the SDD), even at temperatures of 40 °C and at water contents equivalent to humidity conditions of up to 60% RH, is low. This low rate of diffusion of drug in a dispersion at or below the  $T_g$  of the SDD results in the diffusion of drug being the rate-limiting step for drug to crystallize. For such homogeneous fluids near their  $T_g$  and with  $T_g$  values of about 60 °C, the diffusion coefficient of a solute with a size of

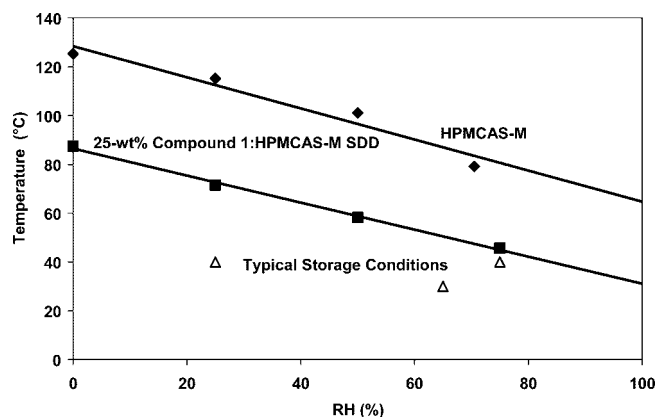


**Figure 6.**  $T_g$  of a 25-wt % Compound 1/HPMCAS-M SDD and HPMCAS-M alone as a function of RH at 25 °C. Lines are least-squares fits to the data. Triangle data points show typical storage conditions.

about 1 nm decreases by about 10-fold for every 10 °C decrease in temperature.<sup>71</sup>

As a result, in this regime (temperature between 30 °C below and 20 °C above the  $T_g$ ; homogeneous dispersion, drug concentration above its solubility in HPMCAS but below about 70 wt %), diffusion of drug is sufficiently slow that it is the rate-limiting step for crystallization; we observe that the time to 5% phase separation for an SDD increases by about 10-fold for every 10 °C increase in the value of  $T_g - T_{\text{storage}}$  ( $T_g$  is the  $T_g$  of the SDD at the storage conditions, and  $T_{\text{storage}}$  is the storage temperature). As a result, we have found that as long as the value of  $T_g - T_{\text{storage}}$  is greater than about 5–30 °C and the SDD is initially homogeneous, less than 5% phase separation is observed over a period of 2 years.<sup>72</sup> The physical stability of SDDs is further illustrated by the data in Table 2, which show that SDDs can be stored for long periods of time with no change in the amorphous nature of the drug in the SDD. This is also evidenced by the appearance of the SDDs in the SEM images (Figure 2). It has been our experience that SEM images are a sensitive measure of low levels of crystallinity—down to 1 wt % or less—allowing more sensitive levels of detection than PXRD. Even more importantly, the dissolution properties of the SDDs, as reflected in their AUC values, show no significant changes over the time of storage. It is anticipated that

(70) “Phase separated” indicates the existence of separate drug-rich and drug-poor phases. However, during the spray-drying process, a concentration gradient develops in the droplet as solvent evaporates, resulting in a slightly higher concentration of polymer at the surface of the solid particle than in the interior. (See Vehring, R. Pharmaceutical Particle Engineering via Spray Drying. *Pharm. Res.* **2008**, 25, 999–1022.) For example, this concentration gradient was measured for 40–60- $\mu\text{m}$  particles of a 25-wt % Compound 1/HPMCAS SDD using infrared absorption in the attenuated total reflectance (ATR) mode, and the surface (outer 600–800 nm) was found to consist of about 12% Compound 1 and 88% HPMCAS. Such SDDs are not phase separated and are termed “homogeneous” dispersions.

**Table 2.** Physical Stability of HPMCAS-Based SDDs Aged at Ambient Conditions

SDD formulation	aging time (years)	observations
25-wt % Compound 1/HPMCAS-M	3.0	no change in $T_g$ , SEM, or dissolution performance
66-wt % Compound 2/HPMCAS-M	2.2	no change in SEM or dissolution performance
10-wt % Compound 7/HPMCAS-H	2.0	no change in SEM or dissolution performance
33-wt % Compound 8/HPMCAS-L	0.7	no change in SEM or dissolution performance
33-wt % Compound 9/HPMCAS-M	0.7	no change in SEM or dissolution performance

HPMCAS-based SDDs will remain physically stable for even longer storage times.

**Aqueous-Solution Properties.** When added to an aqueous solution that simulates fluid present in the duodenum and small intestine, SDDs rapidly dissolve and/or disperse to produce a wide variety of potential species, as shown in Figure 7. For convenience in characterizing and comparing the species formed by various SDDs under various conditions, we have divided these species, based on their size and composition, into the following seven classes: (1) free or solvated drug, (2) drug in bile-salt micelles, (3) free or solvated polymer, (4) polymer colloids, (5) amorphous drug/polymer nanostructures, (6) small aggregates of amorphous drug/polymer nanostructures (termed “nanoaggregates”), and (7) large amorphous particles, referred to in this paper as precipitate. Key to the performance of HPMCAS-based SDDs is the formation of the amorphous drug/polymer nanostructures and small aggregates of these structures (nanoaggregates), as these constitute a stable amorphous, high-energy form of drug that can rapidly dissolve due to their small size (20–300 nm). General size information for these species is given in Figure 7.

The authors believe that drug/polymer nanostructures and nanoaggregates are critical for enhanced oral drug absorption because they (1) rapidly form upon introduction of the SDD to an aqueous solution, (2) produce a free-drug concentration that is enhanced relative to the solubility of crystalline drug, (3) sustain a high free-drug concentration by replacing free

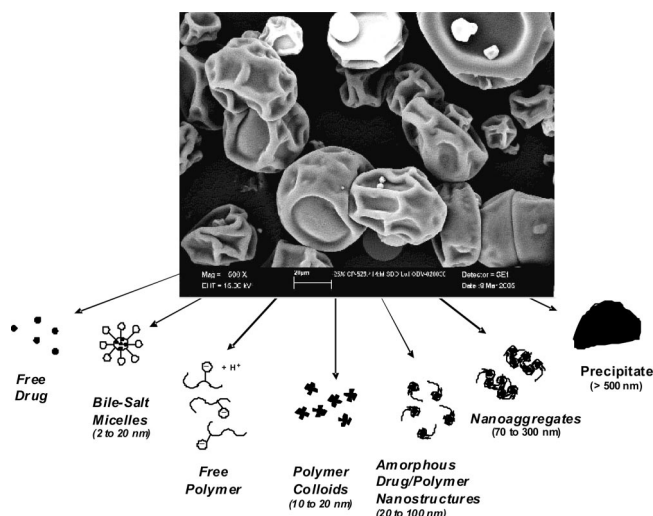


**Figure 7.** Species that form when SDDs are added to aqueous solutions simulating duodenal and intestinal contents.

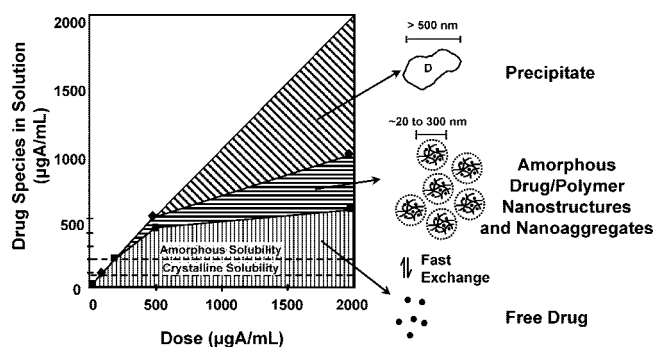
drug as it is absorbed over a biologically relevant time frame,<sup>73</sup> and (4) are stable in aqueous suspension, preventing or inhibiting the conversion of the amorphous high-energy drug form to the low-solubility crystalline form. For simplicity, the drug/polymer nanostructures and nanoaggregates are referred to as “drug/polymer colloids”. These drug/polymer colloids have generally been separated from precipitate using centrifugation and from dissolved species using dialysis. They have been characterized by dynamic light scattering, and their size and structure verified by cryogenic TEM imaging. The amorphous character of the drug present in colloids was verified by lyophilizing the colloid suspensions and analyzing the lyophilized material by PXRD and DSC.

(71) Using the approach introduced by Angell (Angell, C. A. *Strong and Fragile Liquids in Relaxations in Complex Systems*; Nagai, K., Wright, G. B., Eds.; National Technical Information Service, U.S. Department of Commerce: Washington, DC, 1985; p 1), the temperature dependence of the viscosity of glasses can be presented in a  $T_g$ -scaled Arrhenius plot. The minimum slope of the  $\log_{10}$  viscosity versus  $T_g/T$  is for so-called strong liquids. For all real organic, glass-forming materials, the slope at temperatures near  $T_g$  (0.9–1.1-fold the  $T_g$  measured in Kelvin) is at least 2–3-fold this minimum value. [See Wang, L.; Velikov, V.; Angell, C. A. Direct Determination of Kinetic Fragility Indices of Glass-Forming Liquids by Differential Scanning Calorimetry. *J. Chem. Phys.* **2002**, *117*(22), 10184–10192.] This actual slope is equal to the “fragility” of the amorphous material. Taking a conservative estimate of fragility to be 2–3-fold that of the strong-fluid limit, we find that, for a 10 K decrease in temperature from a  $T_g$  value of 60 °C (333 K), viscosity increases between 10-fold and 20-fold. Assuming that the diffusion coefficient of drug in the dispersion decreases inversely proportional to the viscosity, then we would expect the diffusion coefficient of drug in an HPMCAS dispersion with a  $T_g$  near 60 °C to decrease 10–20-fold for every 10 °C decrease in temperature.

(72) The actual rate of phase separation and the corresponding time to 5% phase separation has been measured for many different SDDs over a wide range of storage temperatures—both above and below the  $T_g$  of the dispersion. Based on linear extrapolation of the data for temperatures near or above the  $T_g$  plotted as the  $\log_{10}$  of the time to 5% phase separation versus  $T_g/T_{\text{storage}}$ , the predicted storage temperatures at which the time to 5% phase separation is 2 years are from 5 to 33 °C below the  $T_g$  of the dispersion. This is based on data from HPMCAS dispersions of seven different compounds.

(73) *In vitro* experiments in which the free drug is rapidly removed from suspension or the suspension is rapidly diluted show that the free-drug concentration generally returns to its equilibrium value within 60 s or less.





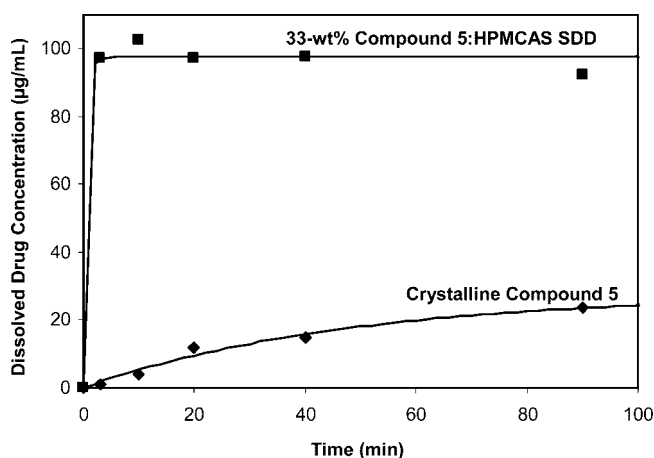
**Figure 8.** Drug species in solution versus drug dose for a 25-wt % Compound 3/HPMCAS-M SDD. Precipitate was separated from the suspensions by centrifugation at 13 000g.

Figure 8 illustrates the relative amount of these various drug species as a function of dosed drug level in the form of a HPMCAS SDD dosed into an aqueous buffer solution (with no bile-salt micelles present), using Compound 3 as an example. At low dose, below the solubility of amorphous drug, the SDD dissolves to form only free drug and free polymer in solution. As the dose of drug as SDD increases to a value above the solubility of amorphous drug, drug/polymer colloids begin to form. As the dose increases, the capacity for the polymer to form these drug/polymer colloids is reached and aggregated drug/polymer colloids begin to form a precipitate. Ideally, this precipitate would be avoided since, though amorphous, it would be expected to dissolve more slowly than the submicron structures. In some cases, this precipitate has been found to be highly labile and can reform drug/polymer colloids upon dilution.<sup>74</sup>

When an SDD is added to an aqueous medium, it dissolves rapidly to form these species. As illustrated in Figure 9, the dissolution rate of SDD particles is at least 2 orders of magnitude faster than that of crystalline drug, completely dissolving within 3 min, whereas the crystalline drug requires more than 100 min to reach its equilibrium solubility. In this experiment, “dissolved drug” includes all species that are not removed by centrifugation at 13 000g or that pass through a 0.45- $\mu\text{m}$  filter, including free drug, drug in micelles, and drug in drug/polymer colloids. Measurement of free drug by NMR spectroscopy showed that the concentration of free drug and drug in micelles provided by the SDD was about 5-fold that provided by the crystalline drug.

Similar results are obtained for SDDs of other compounds as illustrated in Figure 10, which shows the dissolved drug concentration as a function of time for the SDDs and crystalline form of various drugs dosed into MFD solution (dose shown in the figure caption).<sup>75</sup> The data in Figures 9 and 10 also show that drug in these various drug species is stable for long periods of time and does not significantly convert to precipitate—amorphous or crystalline—over the 100–200-min duration of these experiments.

(74) For example, during dissolution testing of SDDs, precipitate can be separated by centrifugation. When fresh dissolution medium is added to the precipitate, additional free drug and drug/polymer colloids are formed.



**Figure 9.** Comparison of dissolution rate of a 33-wt % Compound 5/HPMCAS SDD and crystalline Compound 5. The average particle size of the SDD was  $\sim 1\text{--}10\ \mu\text{m}$ , and that of crystalline Compound 5 was  $\sim 5\text{--}20\ \mu\text{m}$ . The SDD had a dissolution rate constant of greater than  $2\ \text{min}^{-1}$ , whereas crystalline Compound 5 had a dissolution rate constant of  $0.02\ \text{min}^{-1}$ . Test conditions: dosed at  $100\ \mu\text{g/mL}$  into MFD solution at  $37\ ^\circ\text{C}$ ; crystalline drug was dosed with HPMCAS already dissolved in the MFD solution.

The data in Figures 9 and 10 also illustrate that the enhanced drug concentration provided by the SDD relative to crystalline drug is sustained over at least 100 min. This time is on the order of the residence time of the small intestine, about 2–5 h, allowing ample time for drug to be absorbed. For most of the compounds in Figure 10, the dissolved drug concentration provided by the SDD was sustained above that of the crystalline or amorphous compound for at least 20 h (data not shown). Sustained supersaturated drug concentrations are further illustrated in Figure 11, which plots the NMR-visible drug concentration of Compound 1 versus time, as measured by  $\text{F}^{19}$  NMR analysis. The  $\text{F}^{19}$  drug peak integrated to calculate the NMR-visible drug was sharp, having a peak width approximately equal to that of an organic solution of Compound 1. This indicates that the drug species being measured had high mobility and, in this case, corresponds to the sum of free drug and drug in micelles.<sup>76</sup> Drug associated with polymer generally has sufficiently low mobility that its NMR peak width is so broad that it has negligible contribution to the NMR peak area. Such broad NMR peaks are partially due to the larger size of the drug/polymer colloids (20–300 nm) but more importantly due to the solid, highly viscous nature of the amorphous particles (viscosity  $> 10^{10}\ \text{P}$ ).<sup>77</sup> For comparison, the equilibrium solubility of crystalline Compound 1 in this medium is about  $5\ \mu\text{g/mL}$ . Thus, the sum of free-drug and drug-in-micelle concentrations provided by the SDD is about 9-fold that provided by

(75) Approximate particle sizes for the amorphous or crystalline controls consisting of drug alone were amorphous Compound 1,  $1\text{--}10\ \mu\text{m}$ ; crystalline Compound 2,  $2\text{--}5\ \mu\text{m}$ ; amorphous Compound 3,  $1\text{--}10\ \mu\text{m}$ ; crystalline Compound 4,  $5\text{--}50\ \mu\text{m}$ ; amorphous Compound 6,  $1\text{--}10\ \mu\text{m}$ ; crystalline Compound 6,  $5\text{--}70\ \mu\text{m}$ ; and crystalline Compound 9,  $5\text{--}170\ \mu\text{m}$ .

crystalline drug. We have found that for most low-solubility compounds the concentration of drug in micelles,  $C_{\text{micelle}}$ , closely follows the simple relationship

$$C_{\text{micelle}} = V_m K_{m/aq} C_{\text{free}} \quad (1)$$

where  $V_m$  is the volume fraction of micelles,  $K_{m/aq}$  is the micelle/aqueous partition coefficient for the compound, and  $C_{\text{free}}$  is the concentration of free drug. Thus, the NMR-free drug,  $C_{\text{NMR}}$ , is approximately given by the relationship

$$C_{\text{NMR}} = C_{\text{free}}(1 + V_m K_{m/aq}) \quad (2)$$

Using the data in Figures 9–11, the micelle/aqueous partition coefficient for each drug, and these relationships,

the concentrations of various species in solution were calculated for SDDs of Compounds 1 and 3. (Concentrations obtained with amorphous and crystalline forms of Compounds 1 and 3 are shown for comparison.) The results of these calculations are shown in Table 3.<sup>78</sup> The data in Table 3 show that the free-drug concentrations produced by dissolution of the SDDs in MFD solution are 9-fold that of crystalline Compound 1 and 5-fold that of crystalline Compound 3. The SDD free-drug concentration is equal to that of amorphous drug for Compound 1 and slightly more than 2-fold that of amorphous drug for Compound 3. Measurement of free-drug concentrations for SDDs of many

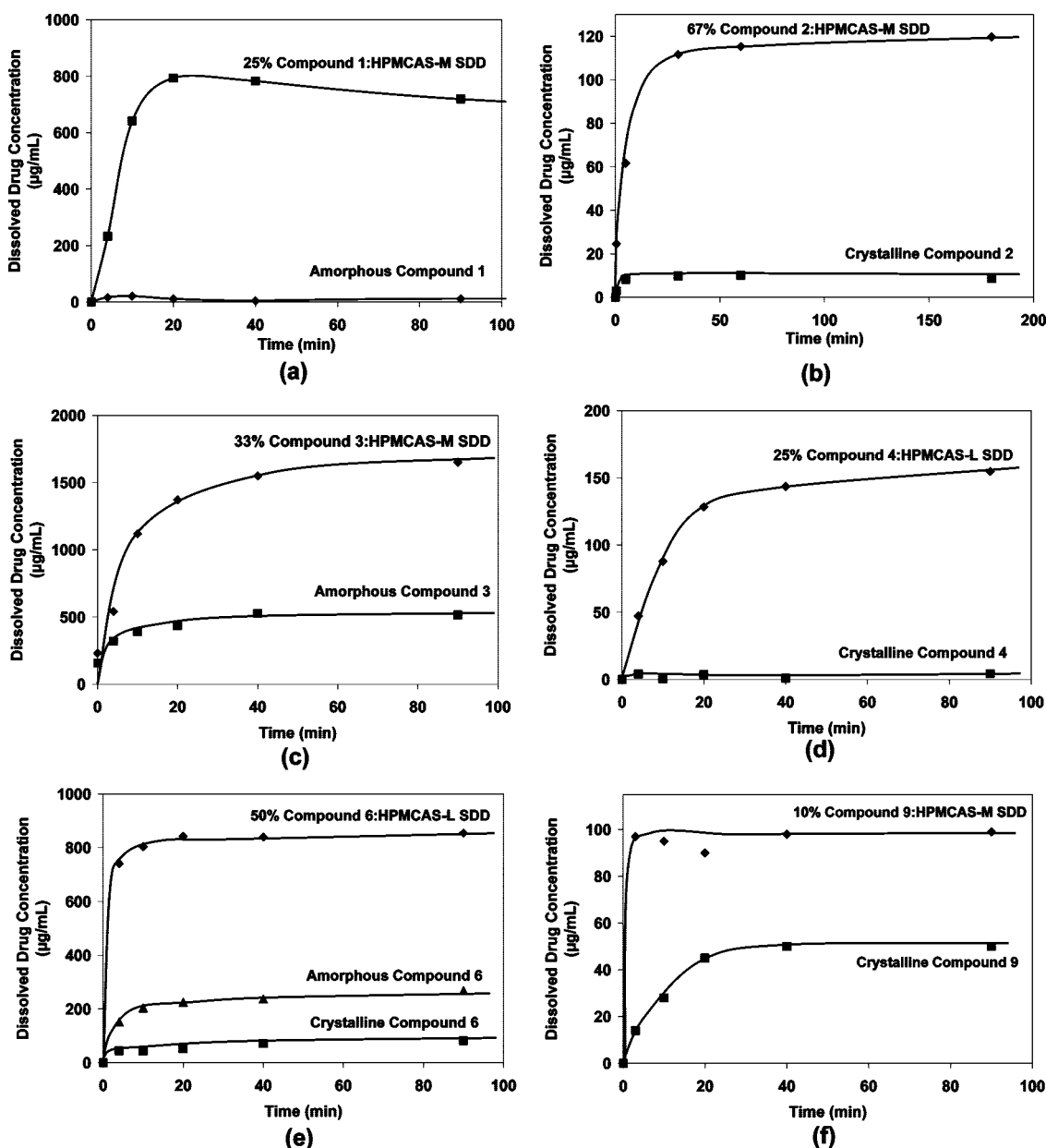


**Figure 10.** Microcentrifuge dissolution data comparing crystalline or amorphous drug alone with the corresponding SDD: (a) 25-wt % Compound 1/HPMCAS-M, dosed at 1000 µg/mL; (b) 67-wt % Compound 2/HPMCAS-M, dosed at 500 µg/mL; (c) 33-wt % Compound 3/HPMCAS-M, dosed at 2000 µg/mL; (d) 25-wt % Compound 4/HPMCAS-L, dosed at 200 µg/mL; (e) 50-wt % Compound 6/HPMCAS-L, dosed at 1000 µg/mL; and (f) 10-wt % Compound 9/HPMCAS-M, dosed at 100 µg/mL. Test conditions: dosed into MFD solution at 37 °C.

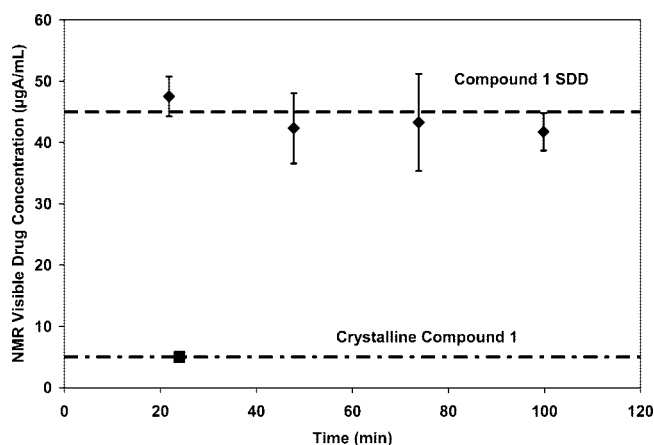


**Figure 11.** NMR-visible drug versus time for a 25-wt % Compound 1/HPMCAS-M SDD. Test conditions: dosed at 1000 µg/mL into 2% MFD solution at 37 °C.

different compounds has yielded values that are in the range of 1–3-fold the amorphous solubility. This enhanced and sustained increase in free drug is the primary driver for enhanced oral absorption.

In addition, enhancement of free drug via SDDs leads to a proportional increase of drug in micelles and a resultant decrease of drug present as “precipitate” (either amorphous or crystalline solids). High levels of drug in micelles promote absorption by shuttling drug across the intestinal mucus boundary layer and by rapidly replacing free drug as it is absorbed. Finally, for SDDs, the majority of drug not “free” or in micelles is present as drug/polymer colloids, rather than as precipitate. Although drug in such colloids is not dissolved, its small size and high free energy should, in

principle, allow it to rapidly dissolve to replace free drug as it is absorbed.<sup>79,80</sup>

**In Vivo Performance.** More than 100 different drugs have been formulated as SDDs and tested in various animal models. SDD absorption enhancement relative to crystalline drug ranges from around 2-fold to near 40-fold. In addition, 21 different drugs have been formulated as SDDs and successfully tested in humans. In all cases where a poorly absorbed control composition was dosed for comparison, the SDD led to a fraction of dose absorbed at least 2-fold that of the control. Figure 12 summarizes the *in vivo* performance of SDDs versus crystalline drug for several drugs in beagle dogs, whereas Figure 13 summarizes results in human clinical studies.

The data in Figures 12 and 13 show that in cases where the crystalline control composition is poorly absorbed, the average enhancement in plasma AUC is around 10-fold for SDDs dosed orally.<sup>81</sup> This enhancement was essentially independent of the absolute AUC value (which is primarily related to the amount of drug dosed).

The breadth of applicability of HPMCAS-based SDDs is illustrated in Figure 14. Plotted here are more than 130 drug candidates that have been formulated as HPMCAS SDDs, as a function of the  $T_m/T_g$  (K/K) ratio and log  $P$  value of the compounds. It has been found that the  $T_m/T_g$  ratio provides an indication of the propensity for the compound to crystallize. Compounds that have high  $T_m$  values have a strong tendency to crystallize due to the large thermodynamic driving force, and compounds with low  $T_g$  values have a low kinetic barrier for molecular diffusion (that is, their diffusion coefficient at a given temperature is relatively high). Thus, the  $T_m/T_g$  ratio combines both a thermodynamic parameter ( $T_m$ ) and a kinetic parameter ( $T_g$ ). We have found that SDDs made from compounds with high  $T_m/T_g$  ratios generally crystallize more rapidly (at a given drug loading and temperature) than SDDs made from compounds with low  $T_m/T_g$  values. Such compounds with high  $T_m/T_g$  ratios (for example, due to low  $T_g$  values) can be stabilized by dispersing the compound in the high- $T_g$  HPMCAS polymer. However, at a given drug loading, the  $T_g$  of the SDD generally decreases with decreasing  $T_g$  of the drug. As a result, to maintain equivalent stability, the drug loading in the SDD must be lowered with decreasing drug  $T_g$  or increasing drug  $T_m/T_g$  ratio. (This trend is reflected in Figure 14.)

(76) The mixed micelles formed by the taurocholate and lecithin in the MFD solution are reported to be about 4–6 nm in diameter (see Bray, J. J.; Cragg, P. A.; MacKnight, A. D. C.; Mills, R. G.; Taylor, D. Digestive System. In *Lecture Notes on Human Physiology*. Blackwell Publishers: Oxford, England, 1999; Chapter 17, p 508); this is consistent with the results of our light-scattering experiments, which showed diameters of about 5–10 nm. Drug present in such small, fluid structures is expected to yield sharp NMR peaks due to their high mobility. Consistent with this, plots of the drug NMR peak area versus micelle volume for excess crystalline drug equilibrated with solutions with varying micelle concentrations were linear over the 0.5–4.0 vol % range for most drugs measured and the y intercept was approximately the crystalline solubility.

(77) For at least one drug we have tested (not one of the drugs described in this paper) that is a viscous oil at 37 °C, drug in drug/polymer colloids is NMR-visible and displays NMR peaks much broader than those of the same drug in bile-salt/lecithin micelles.

(78) The concentration of NMR-visible drug observed at long times (1–20 h) for SDDs and amorphous drug particles is similar for many compounds. This is one reason that we believe that the drug/polymer colloids formed by the HPMCAS SDDs can be thought of as stabilized amorphous drug colloids. This also suggests that there is not a strong interaction between the micelles in MFD solution and the drug/HPMCAS colloids.

(79) Curatolo, W. J.; Shanker, R. M.; Babcock, W. C.; Friesen, D. T.; Nightingale, J. A. S.; Lorenz, D. A. Pharmaceutical Compositions Providing Enhanced Drug Concentrations. U.S. Patent Application No. 2002/0006443A1, January 17, 2002.

(80) It is interesting to note that amorphous drug/HPMCAS colloids can be formed without first forming SDDs. For example, HPMCAS can be predissolved in dissolution medium and drug added in a high-energy form—for example, amorphous drug, a soluble salt, or a solution—and drug/polymer colloids are observed to form and the concentration of dissolved drug remains at a supersaturated level.

(81) The enhancement over crystalline drug was, of course, lower in cases where the crystalline drug control was moderately well absorbed.



**Table 3.** Concentrations of Drug Species When Amorphous Drug, Crystalline Drug, or HPMCAS-SDD is Dosed into MFD Solution at 37°C

formulation	dose ( $\mu\text{g/mL}$ )	partition coefficient	concentration of drug-containing species ( $\mu\text{g/mL}$ )**			
			free drug	micelles*	drug/polymer colloids	precipitate
25-wt % Compound 1 SDD	1000	33 000	0.08	13	717	270
amorphous Compound 1			0.08	13	0	987
crystalline Compound 1			0.009	1.5	0	998
33-wt % Compound 3 SDD	2000	400	400	800	450	350
amorphous Compound 3			180	360	0	1460
crystalline Compound 3			80	160	0	1760

\* A value of 0.005 for  $V_m$  for the mixed micelles in MFD solution was used to calculate the drug concentration in micelles.

\*\* Concentrations are the drug content of each species. For example, 717  $\mu\text{g/mL}$  of drug/polymer colloids also contain polymer. Thus, if the colloids were 25-wt % drug, the total colloid concentration would be 2868  $\mu\text{g/mL}$ .

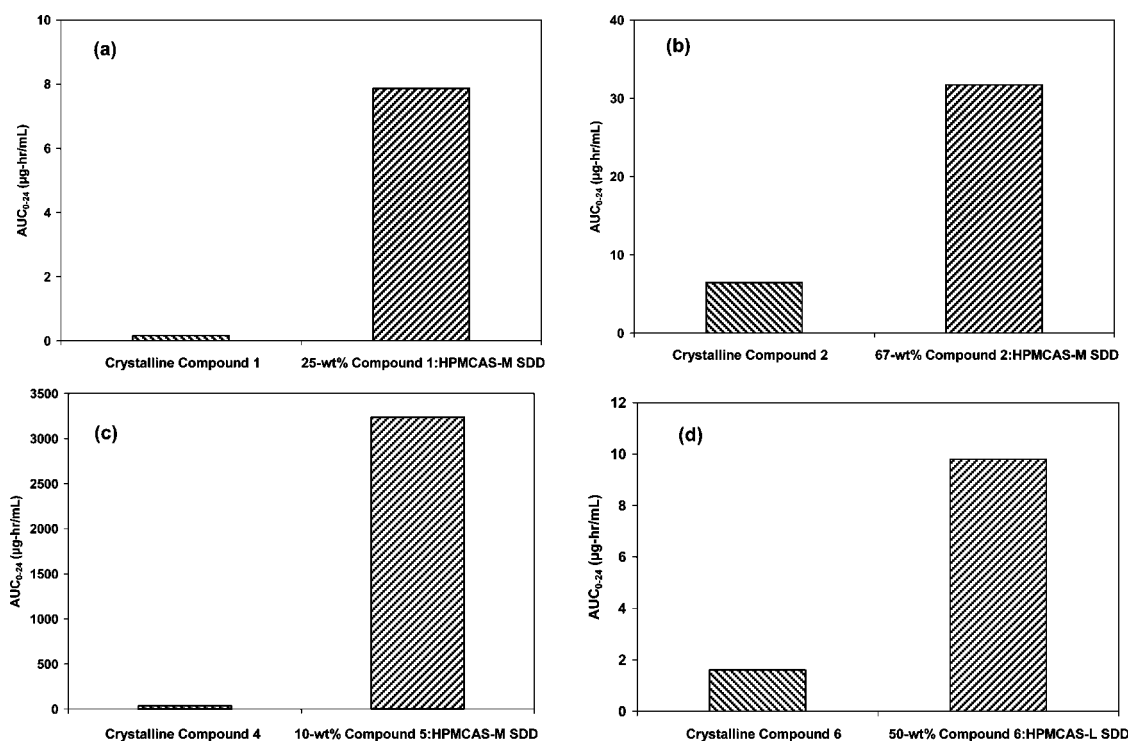


**Figure 12.** Comparison of canine *in vivo* exposure for crystalline drug and SDDs: (a) 25-wt % Compound 1/ HPMCAS-M SDD (crystalline particle size  $\sim 90 \mu\text{m}$ , AUC = 0.44, standard deviation (SD) = 0.27,  $n = 6$ ; SDD AUC = 7.9, SD = 3.0,  $n = 6$ ); (b) 67-wt % Compound 2/HPMCAS-M SDD (crystalline particle size  $\sim 2\text{--}5 \mu\text{m}$ , AUC = 6.5, SD = 3.6,  $n = 4$ ; SDD AUC = 31.8, SD = 18.6,  $n = 4$ ); (c) 10-wt % Compound 4/HPMCAS-M SDD (crystalline particle size  $\sim 5\text{--}50 \mu\text{m}$ , AUC = 34, SD = 17,  $n = 3$ ; SDD AUC = 3240, SD = 120,  $n = 3$ ); and (d) 50-wt % Compound 6/HPMCAS-L SDD (crystalline particle size  $\sim 5\text{--}70 \mu\text{m}$ , AUC = 1.7, SD and  $n$  unknown; SDD AUC = 9.8, SD and  $n$  unknown). All data collected from beagle dogs.

The log  $P$  value is a standard measure of the lipophilicity of a compound. Compounds with high log  $P$  values (for example, greater than about 4) are very hydrophobic and tend to have extremely low water solubilities (often less than 1  $\mu\text{g/mL}$  when their melting points are above about 100 °C) and low propensities for wetting when placed into water. As the data in Figure 14 show, the HPMCAS-based SDD technology is applicable to compounds covering a structurally diverse range of physicochemical properties.

Work in formulating and testing the wide range of compounds has shown that SDD properties of compounds are, in general, related to their position on the map of  $T_m/T_g$

ratio versus log  $P$ . As shown in Figure 14, this has allowed us to divide the compounds into four groups based on their position on this physical property map. The specific locations of the boundaries drawn for these four regions are somewhat arbitrary but reflect two general trends: (1) as the log  $P$  of the compound increases, the dissolution rate of the SDD decreases; and (2) as the  $T_m/T_g$  ratio of the compound increases, the physical stability of the SDD decreases. Both of these potentially negative SDD attributes can be mitigated by decreasing the drug loading in the SDD. Thus, the maximum SDD drug loading that leads to acceptable physical stability and dissolution rate is generally high (greater than

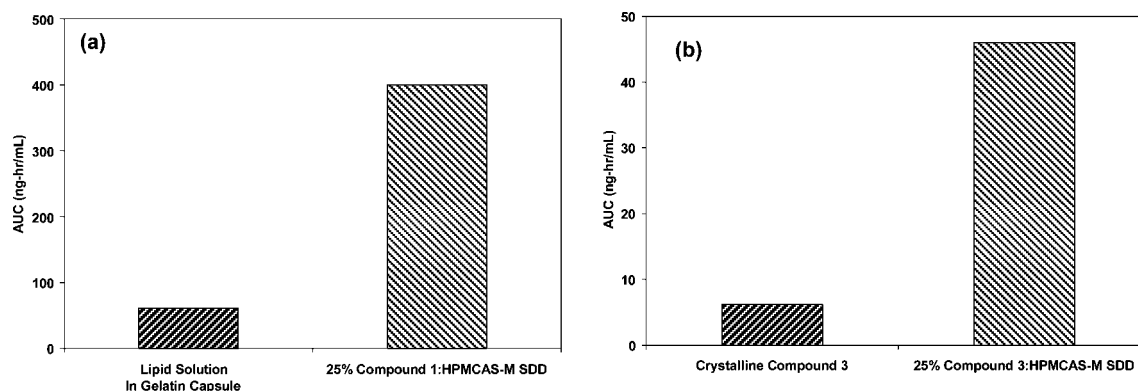


**Figure 13.** Comparison of human *in vivo* exposure for crystalline drug (or crystalline drug in gelatin capsule) and SDDs: (a) 25-wt % Compound 1/HPMCAS-M SDD (dosed at 30 mg fasted) and (b) 25-wt % Compound 3/HPMCAS-M SDD (dosed at 300 mg fasted).

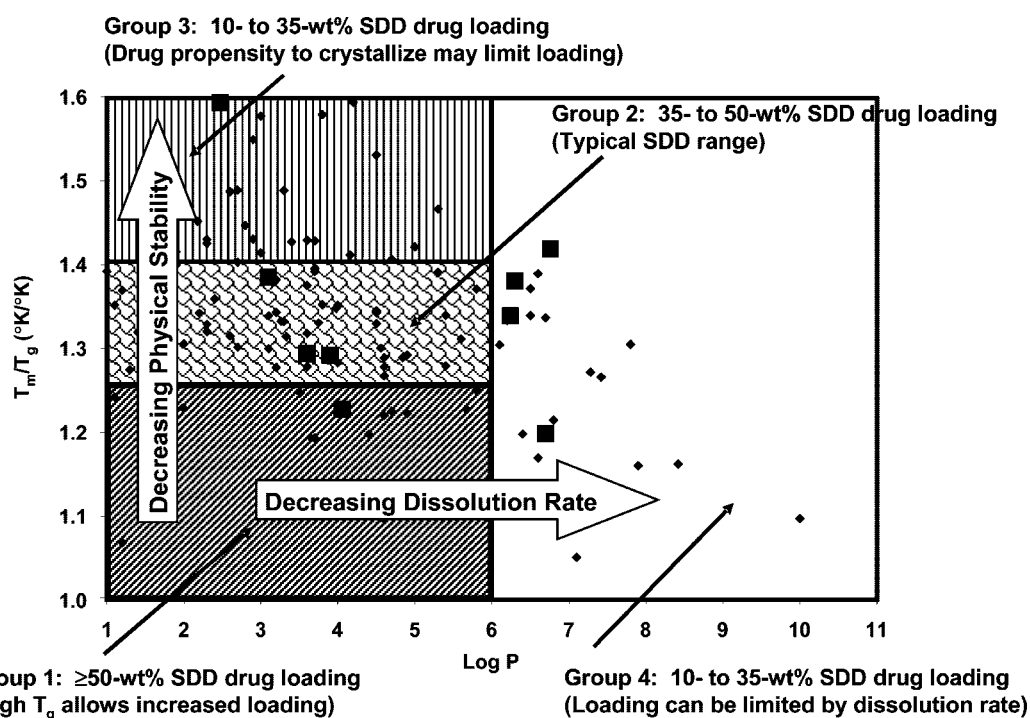


**Figure 14.**  $T_m/T_g$  versus  $\log P$  for 139 low-solubility compounds successfully formulated as SDDs (which achieved supersaturation in *in vitro* dissolution tests). The points labeled with large squares are the example compounds used throughout the article.

50 wt %) for compounds at the lower left of this plot and progressively decreases for compounds with high  $\log P$  or  $T_m/T_g$  values. These trends are reflected in the four regions depicted in Figure 14. The first group, Group 1, consists of compounds with relatively low  $T_m/T_g$  ratios ( $<1.25$  K/K) and low to moderate  $\log P$  values (less than about 6); these compounds generally can be successfully formulated as SDDs with high drug loadings (for example, 50 wt % or more) while maintaining acceptable physical stability and rapid dissolution rates.

Compounds in Group 2 have somewhat higher  $T_m/T_g$  ratios (1.25–1.4). HPMCAS-based SDDs with somewhat

lower drug loadings (for example, 35–50 wt % are normally needed to ensure the SDD has sufficient physical stability.

Compounds in Group 3 have even higher  $T_m/T_g$  values (greater than 1.4). Compounds in this region normally require drug loadings between 10 and 35 wt % and, particularly at the high end of  $T_m/T_g$  values, often require packaging to avoid ingress of water or storage under reduced humidity conditions to maintain physical stability.

Finally, for Group 4 compounds, which have very high  $\log P$  values (greater than about 6), SDDs with drug loadings in the 10–35 wt % range are normally required to have acceptably rapid dissolution rates. The extreme lipophilicity

and very low aqueous solubility of compounds in this region lead to SDDs that dissolve slowly if drug loading is high. Despite this tendency, SDDs with reduced drug loadings perform well *in vivo*. Specifically, a 25-wt % SDD of Compound 1 has shown excellent oral absorption in clinical studies.

## Conclusion

HPMCAS-based SDDs have been prepared from low-solubility drug candidates having a wide range of physicochemical properties. These SDDs provide significant enhancements in oral absorption of poorly water-soluble compounds by rapidly providing a free-drug concentration

well in excess of their crystalline solubilities and maintaining these enhanced concentrations for long times by forming stable amorphous drug/polymer nanostructures in the intestinal lumen. The composition and resulting physicochemical properties of HPMCAS are responsible for the formation of these structures that enhance bioavailability. Furthermore, the high  $T_g$  of the HPMCAS-based SDDs, combined with the homogeneous, single amorphous phase nature of the SDD (a result of the spray-drying process used to form the SDDs), results in physically stable formulations that have shelf lives of more than 2 years under standard storage conditions.

MP8000793